NASA TECHNICAL NOTE

NASA TN D-4698

NASA TN D-4698

PERFORMANCE CHARACTERISTICS OF 15 kVA HOMOPOLAR INDUCTOR ALTERNATOR FOR 400 Hz BRAYTON-CYCLE SPACE-POWER SYSTEM

by Richard A. Edkin, Martin E. Valgora, and Dennis A. Perz

Lewis Research Center
Cleveland, Ohio

NATIONAL AERONAUTICS AND SPACE ADMINISTRATION • WASHINGTON, D. C. • AUGUST 1968

PERFORMANCE CHARACTERISTICS OF 15 kVA HOMOPOLAR INDUCTOR ALTERNATOR FOR 400 Hz BRAYTON-CYCLE SPACE-POWER SYSTEM

By Richard A. Edkin, Martin E. Valgora, and Dennis A. Perz

Lewis Research Center
Cleveland, Ohio

NATIONAL AERONAUTICS AND SPACE ADMINISTRATION

For sale by the Clearinghouse for Federal Scientific and Technical Information
Springfield, Virginia 22151 – CFSTI price $3.00

ABSTRACT

The measured performance of a 15 kVA homopolar inductor alternator is presented and compared with design goals. Test results include alternator saturation, voltage unbalance, harmonic analysis, short circuits, machine reactances, and time constants. The following overall performance was obtained: maximum continuous output, 22.5 kVA; peak efficiency, 0.918 at 11.25 kVA; and efficiency at rated 15 kVA output, 0.915.

PERFORMANCE CHARACTERISTICS OF 15 kVA HOMOPOLAR INDUCTOR ALTERNATOR FOR 400 Hz BRAYTON-CYCLE SPACE-POWER SYSTEM

by Richard A. Edkin, Martin E. Valgora, and Dennis A. Perz

Lewis Research Center

SUMMARY

The measured performance of a 15 kilovolt ampere homopolar inductor alternator is presented and compared with design goals. Test results include alternator saturation, voltage unbalance, harmonic analysis, short circuits, machine reactances, and time constants.

The following overall performance was obtained: maximum continuous output, 22.5 kilovolt amperes; peak efficiency, 0.918 at 11.25 kilovolt amperes; and efficiency at rated 15 kilovolt amperes, 0.915.

INTRODUCTION

A two-shaft Brayton-cycle turboalternator electric-power system for space application is being investigated at the Lewis Research Center (refs. 1 to 5). This power system has a compressor and turbine on a high-speed shaft and an alternator with a second turbine on a lower-speed shaft. The Brayton thermodynamic cycle is a closed loop using argon as the working fluid.

One of the main objectives of present investigations of the Brayton power system is the determination of individual component performance characteristics. It is the purpose of this paper to present an experimental evaluation for one of these components, the alternator.

This alternator is a homopolar inductor. Some of its unique design features are discussed in reference 6. This particular type of alternator is suitable for use in a space-power system because of its expected high reliability in severe environments, its high efficiency, and its capability of operating at high rotative speeds. A comprehensive

study of this type of machine for application to space-electric power systems is presented in reference 7.

Extensive tests were conducted at the Lewis Research Center on an experimental alternator for the 400 hertz Brayton-cycle power system. This experimental alternator was designed to be electromagnetically and thermally equivalent to the prototype alternator. But whereas argon gas bearings will be used in the prototype, oil-lubricated bearings were used in the experimental alternator in order to simplify the electrical testing.

In this report, results of measurements of alternator saturation, efficiency, harmonic analysis, short circuits, voltage unbalance, machine reactances, and time constants are compared with design goals. With this information, it is possible to predict alternator behavior in the Brayton-cycle electrical power system under transient and steady-state conditions.

SYMBOLS

I_a	armature current
I_F	field current
L-L	line-to-line
L-N	line-to-neutral
PU	per unit
R_a	armature resistance
rms	root mean square
T_a	armature short-circuit time constant
T'_d	direct-axis transient time constant
T''_d	direct-axis subtransient time constant
T'_{do}	direct-axis open-circuit time constant
V_F	field voltage
X_d	direct-axis synchronous reactance
X'_d	direct-axis transient reactance
X''_d	direct-axis subtransient reactance
X_0	zero sequence reactance
X_2	negative sequence reactance
α	switching angle

DESCRIPTION OF ALTERNATOR

This homopolar inductor alternator is rated at 12 000 rpm, is oil cooled, and is brushless. The rated continuous output is: 15 kilovolt amperes, 12 kilowatts, 0.8 lagging power factor, 3-phase, 41.7 amperes, and 120/208 volts at 400 hertz.

Figure 1 is a photograph of the experimental alternator, and figure 2 is a sectional view.

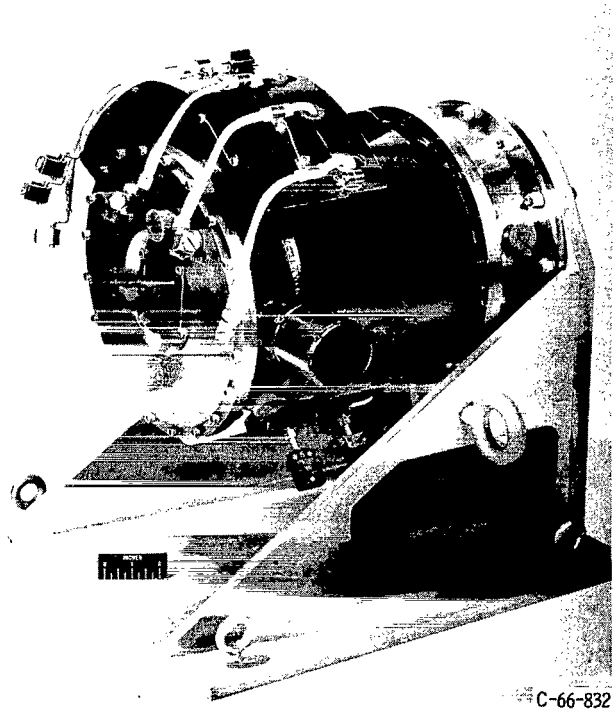

Figure 1. - Experimental alternator.

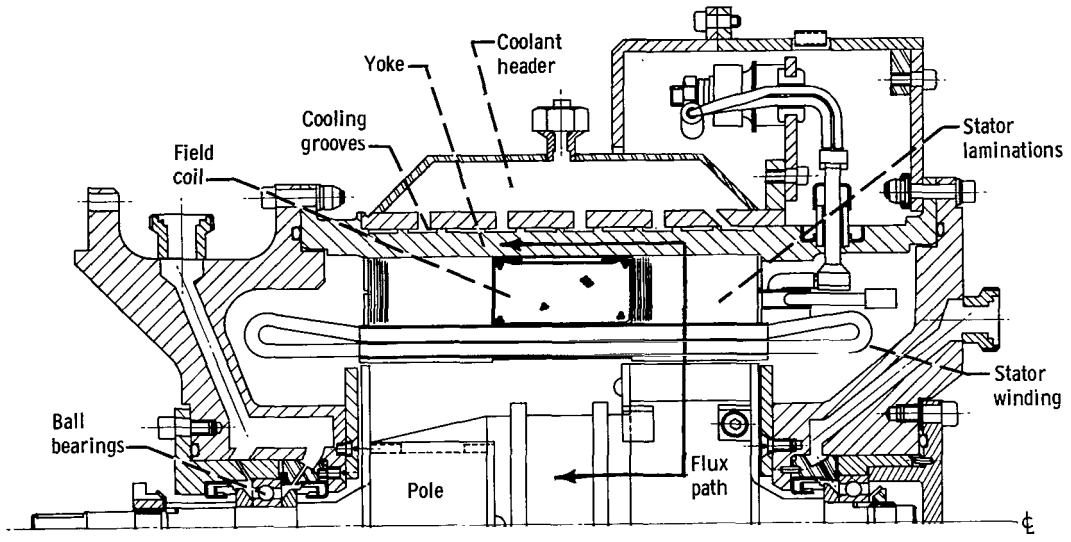

Figure 2. - Sectional view of experimental alternator.

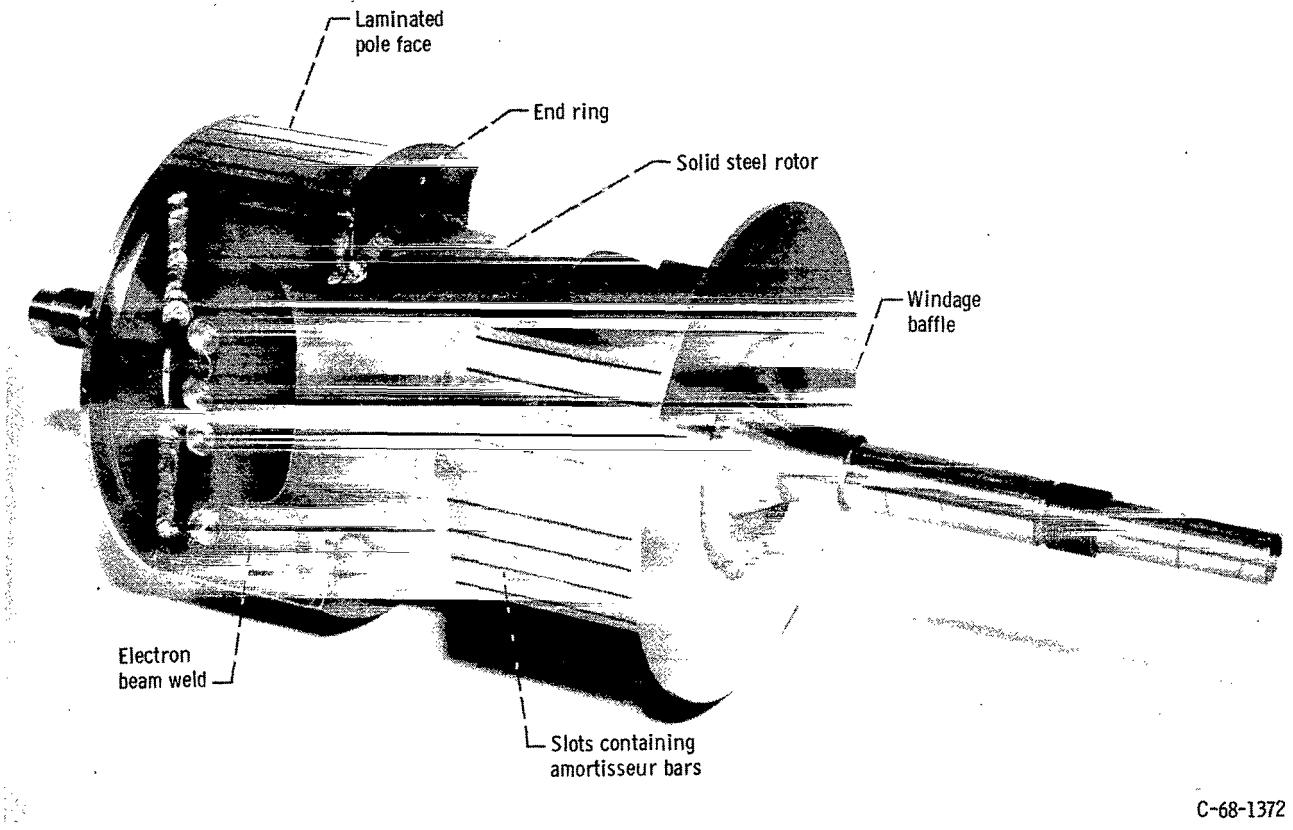

Figure 3. - Experimental alternator rotor. Rotor outside diameter at poles, 5.2 inches (13.2 cm).

The inductor alternator is a synchronous machine that is unconventional in that no field windings are located on the rotor. This construction eliminates rotating field windings, brushes, and slip rings which are undesirable at high rotative speeds and for space environment applications. As a result, the inductor alternator is mechanically simpler than a conventional alternator, and probably has greater life and reliability.

The 4-pole alternator rotor (fig. 3) has two special features, viz., windage baffles and laminated pole tips electron-beam welded to the solid AISI 4620 steel rotor. These features reduce the alternator losses and therefore improve the efficiency.

Damper windings are installed in the pole tips.

APPARATUS AND PROCEDURE

A schematic diagram of the basic components in the test setup is depicted in figure 4. A 3-phase induction dynamometer was used to drive the experimental alternator

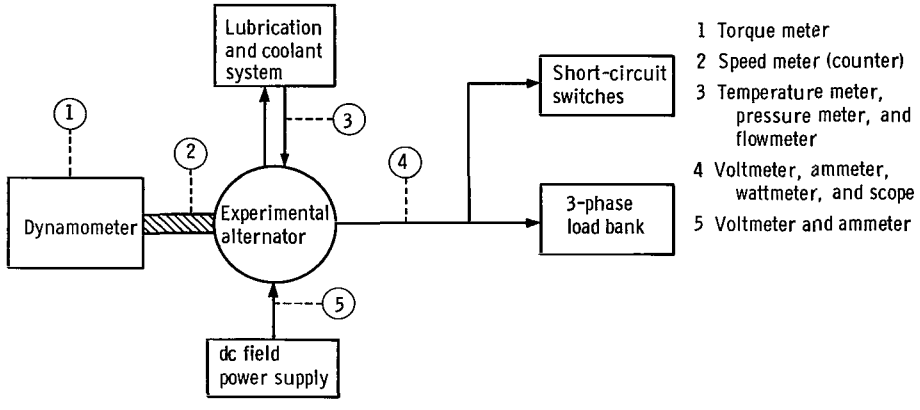

Figure 4. - Schematic diagram of test setup.

at 12 000 rpm. The alternator field was separately excited by a regulated dc power supply. The lubrication and coolant system controlled the alternator inlet oil (specification MIL-L-7808) temperature within $\pm 2.8^{\circ}$ C of the desired temperature for each test and provided preheating capability. A 3-phase load bank was used to apply resistive and reactive loads on the alternator. Short circuit switches were used to apply single-phase, line-to-line, and 3-phase faults on the machine as desired.

Instrumentation

Figure 4 indicates where the instrument sensors were installed in the test setup. The basic parameters monitored or measured included: (1) shaft torque, (2) speed, (3) terminal voltage, (4) line current, (5) power, (6) field current, (7) field voltage, (8) stator temperatures, (9) coolant temperature, (10) coolant inlet pressure, and (11) coolant inlet flow rate.

Figure 5 is a photograph of the instrumentation in the control room of the test facility. Specifications for these instruments are given in the appendix. Prior to their

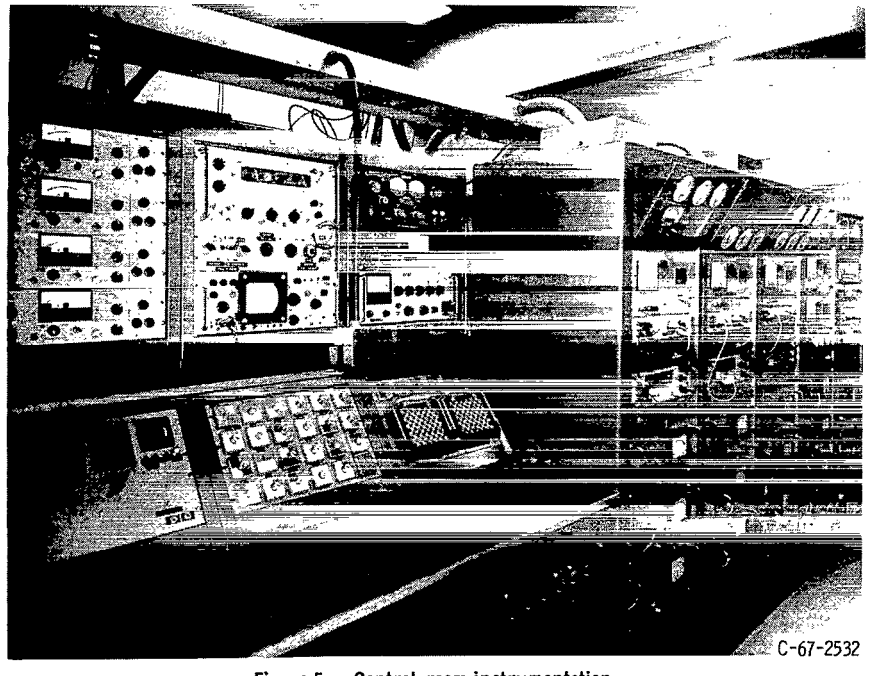

Figure 5. - Control-room instrumentation.

use, the specific instruments required for each test were calibrated to 1 percent of full scale, or better, against a standard accurate to 0.25 percent.

Procedure

Table I lists the design goals of the Brayton electrical system. Unless otherwise indicated in this report, the alternator test procedure was based on approved methods

TABLE I. - DESIGN GOALS OF BRAYTON ELECTRICAL SYSTEM (REF. 11)

Alternator efficiency	(1) Maximum at 11.25-kVA output (2) Maximized for range of 5- to 15-kVA output (excluding bearing losses)	
Harmonic distortion for linear loads (line-to-neutral voltage)	(1) Maximum individual harmonic, <3 percent for any load (2) Total harmonic content, <7 percent at 1.0 power factor from 1.2- to 12-kW load	
Voltage unbalance for 1.0 power factor loads	Load	Maximum unbalance, percent
	0 - 0 - 1/3	2
	0 - 0 - 2/3	4
	1/3 - 2/3 - 1/3	2
	1/3 - 1 - 1/3	4
	2/3 - 2/3 - 1	2
Short-circuit capacity (for minimum of 5 sec)	Short circuit	Minimum current, per unit
	3-phase	3
	Line to neutral	3
Overload, after temperatures stabilized at rated load	(1) 1.5-per-unit load for 2 min (2) 2.0-per-unit load for 5 sec	
Alternator stator temperature	Maximum hot-spot temperature, 180° C	

described in reference 8. For all testing, alternator load power factors are lagging from zero to unity.

RESULTS AND DISCUSSION

Saturation

Alternator saturation curves were experimentally determined for various load conditions. Figure 6(a) shows curves for open-circuit, zero-power-factor, and 3-

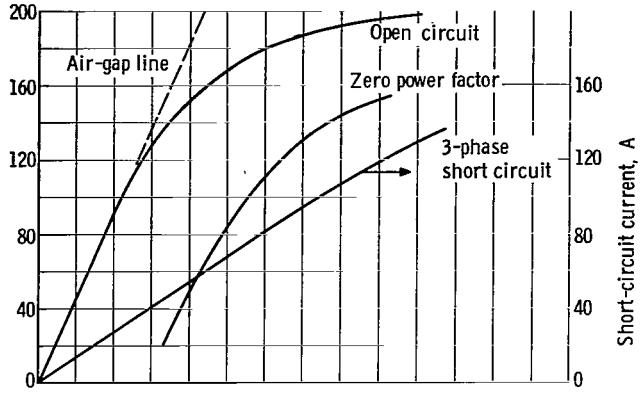

(a) Open circuit, zero power factor, and short circuit.

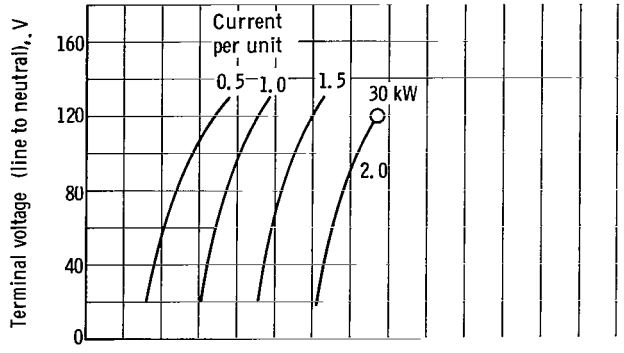

(b) Load saturation curves with unity power factor loads.

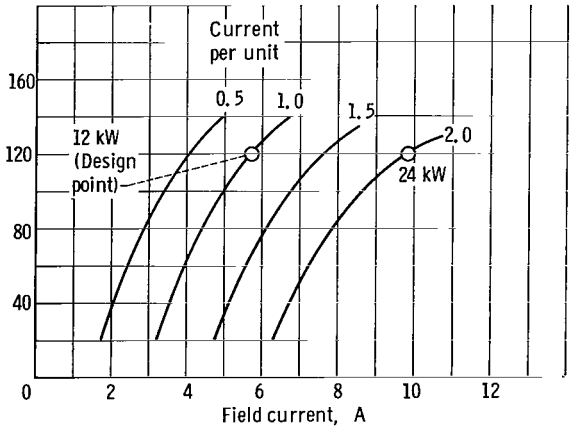

(c) Load saturation curves with 0.8 lagging power factor loads.

Figure 6. - Saturation characteristics of 15-kilovolt-ampere Brayton-cycle alternator. Current of 1 per unit equivalent to 41.7 amperes.

phase short-circuit operation. The open-circuit curve shows that a minimum field excitation of 2.75 amperes is required to generate rated voltage. The zero-power-factor curve was obtained by varying the reactive load and increasing the field current to obtain constant rated armature current. At zero power factor, a field excitation of 6.45 amperes is necessary to generate rated voltage.

For short-circuit saturation, a balanced 3-phase fault was applied at the alternator terminals and an x-y recording of short-circuit current (rms value) as a function of field current was obtained. For this test the external lead resistance was 0.005 ohm per phase. The short-circuit curve is almost linear, indicating negligible saturation and showing that the short-circuit armature current is directly proportional to the field current. These data also demonstrate that this alternator has the capability of delivering 3 per-unit current (125 A) to a balanced 3-phase short circuit. The duration of the short circuit during this test was minimized in order to avoid excessive overheating of the alternator. However, the 3 per-unit current was present for at least 5 seconds.

Families of load saturation curves at unity and 0.8 power factor are illustrated in figures 6(b) and (c). An examination of the data with unity power factor load shows that the alternator has the electromagnetic capacity to generate 30 kilowatts of electrical power at rated voltage without significant saturation. In figure 6(c) the saturation curves with 0.8 power factor load demonstrate that the alternator has the electromagnetic capacity to deliver twice its rated output with low saturation. These data indicate that the alternator is conservative in design.

Losses

The losses listed were individually measured, so that alternator efficiency could be determined from the separation-of-losses method: (1) armature copper, (2) field copper, (3) open circuit core, (4) windage, and (5) stray load. The measured losses are tabulated in table II along with final design values. Bearing friction is not included, because special oil-lubricated bearings were used in the experimental alternator.

The losses were measured for 93.4° C (design) and 26.7° C inlet coolant temperatures. The temperature of 26.7° C was the lowest off-design temperature that the test rig could maintain. By measuring losses at this off-design temperature, it was possible to compare efficiency curves for two different coolant temperatures.

Armature copper. - Figure 7(a) shows curves for armature copper loss ($3I_a^2 R_a$) at 26.7° and 93.4° C coolant temperatures. Since the armature resistance is constant at a specific temperature, the armature loss varies as the square of the armature current. At the design temperature (93.4° C) and rated armature current, the armature copper

TABLE II. - EFFICIENCY[a]

[Argon in cavity; inlet coolant temperature, 93.4° C; power factor, 0.8 (lagging).]

Conditions:				
Cavity pressure, psia	6		10.5	
Output,				
kVA	11.25		15	
kW	9		12	
Losses, kW	Test	Final design	Test	Final design
Armature copper	0.150	0.154	0.277	0.276
Field copper	.097	.157	.135	.206
Core	.320	.190	.320	.200
Windage	.061	.150	.107	.220
Stray load	.170	.1375[b]	.270	.190[b]
Total losses	.798	.7885	1.109	1.092
Efficiency, percent	91.8	91.9	91.5	91.6

[a]Bearing loss not included.

[b]Pole face loss included.

loss is 0.277 kilowatt. The experimental data at 15 kilovolt amperes is within 0.4 percent of the calculated design values given in table II.

Field copper. - Curves of field loss ($V_F I_F$) as a function of alternator output are presented in figure 7(b). At rated load (12 kW) with a coolant temperature of 93.4° C, the field loss is 0.135 kilowatt. The field of this machine is located on the stator. Heat removal is easier than in a rotor field, and the field loss is reduced.

The calculated design value for this loss is 34.5 percent greater than the test value. This difference indicates that the actual field excitation requirements were less than expected.

Open-circuit core. - Figure 7(c) is a plot of open-circuit core loss as a function of the rms value of the line-to-neutral terminal voltage. Core loss varies approximately as the voltage squared. At rated terminal voltage, the loss is 0.320 kilowatt. Comparison of experimental and calculated values of core loss at rated voltage reveals that the test value is significantly higher. Harmonic analysis demonstrated that high-frequency voltage harmonics were present. These harmonics contribute to the iron losses. These harmonic data are presented later in this report.

Windage. - Windage losses are 51.4 percent lower than design predicted indicating that rotor design and windage baffles provide more effective reduction of these losses

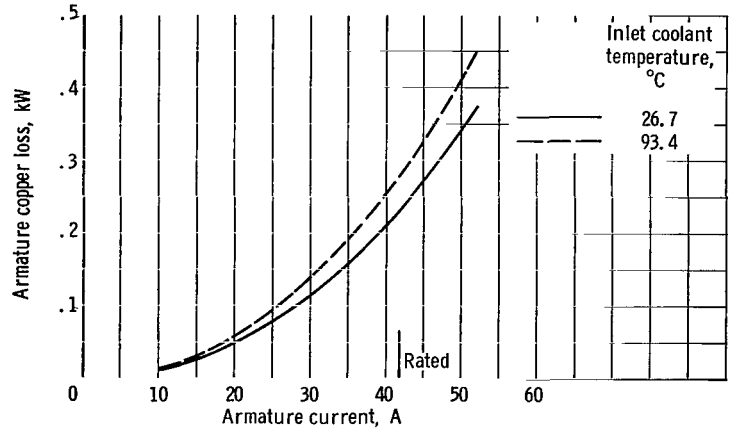

(a) Armature copper loss.

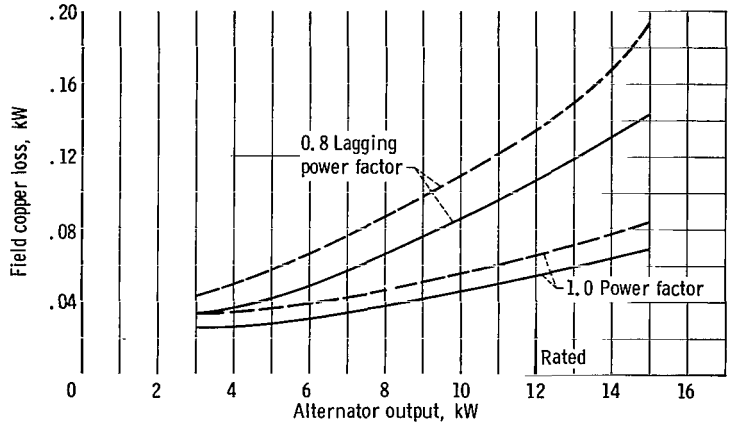

(b) Field copper loss.

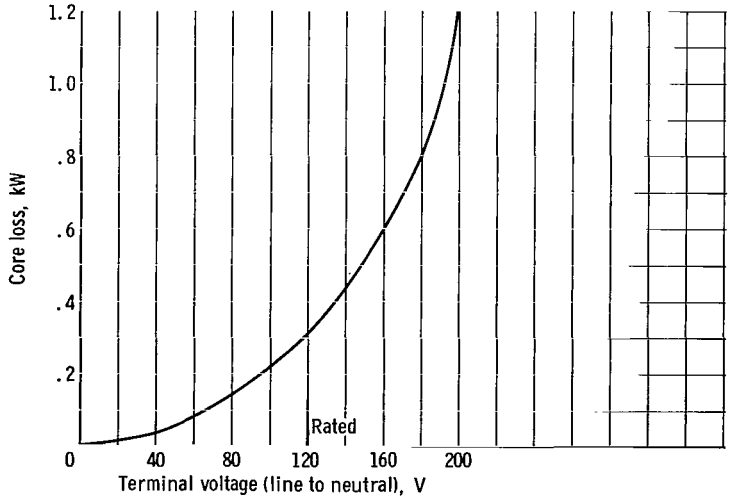

(c) Open-circuit core loss.

Figure 7. - Losses in 15-kilovolt-ampere Brayton-cycle alternator.

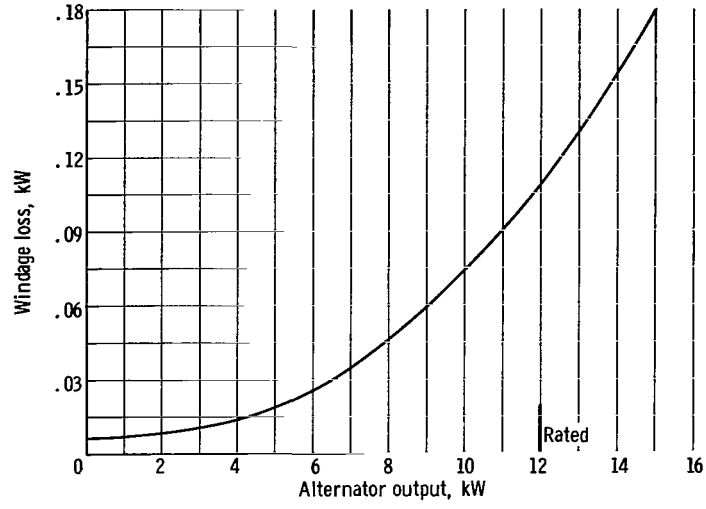

(d) Windage loss at 12 000 rpm. Argon in cavity.

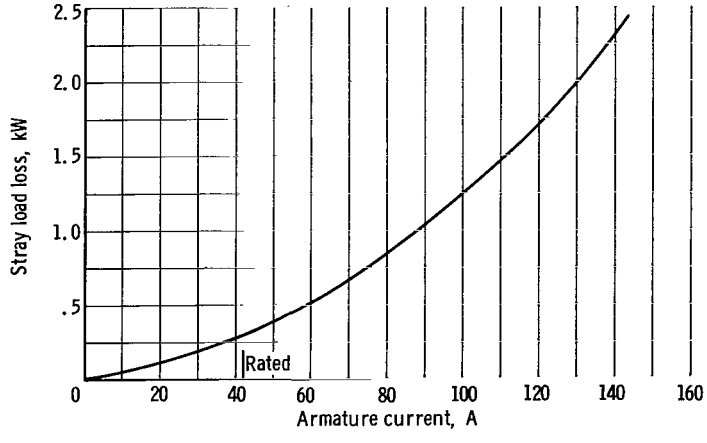

(e) Stray load loss.

Figure 7. - Concluded.

than anticipated. Figure 7(d) shows the variation in windage loss with alternator load; windage loss is 0.107 kilowatt at rated load.

Stray load. - Stray load loss (fig. 7(e)) consists of pole-face losses plus the hysteresis and eddy current losses produced by the armature current. Stray load loss was experimentally determined by applying a balanced 3-phase short circuit on the alternator. Armature copper, windage, bearing, and seal friction losses were subtracted from the total short circuit losses. The resulting stray load loss was 0.270 kilowatt. This value exceeded the predicted loss by 29.6 percent.

Efficiency

Alternator efficiency was calculated from the equation

$$\text{percent efficiency} = \frac{\text{power output}}{\text{power output + losses}} \times 100$$

The efficiency curve (fig. 8(a)) for a 0.8 lagging power-factor load has a peak of 91.8 percent for an output of 9 kilowatts (11.25 kVA). The curve is relatively flat between 4 kilowatts (5 kVA) and 12 kilowatts (15 kVA). This performance satisfies a design goal for the alternator (table I). At rated output the efficiency is 91.5 percent. The efficiency is high and almost constant in the expected normal operating region (9 to 12 kW) for the Brayton alternator.

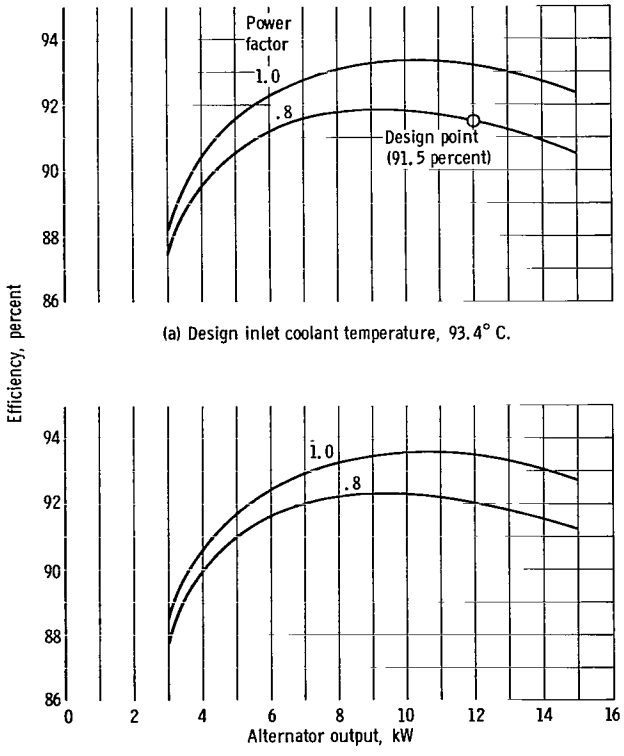

Figure 8. - Efficiency of 15-kilovolt-ampere Brayton-cycle alternator. Bearing loss not included; inlet coolant flow rate, 1.66 gallons per minute (6.3×10^{-3} m^3/min).

For the same operating region, efficiency with unity power-factor load is higher than the efficiency with an 0.8 lagging power-factor load by more than one percentage point. Higher efficiency is the result of smaller armature copper, field copper, and stray load losses. Design and experimental values of efficiency are compared in table II.

Figure 8(b) shows efficiency curves for an off-design inlet coolant temperature of 26.7° C. At rated load an increase in efficiency of 0.5 percent is obtained. Efficiency is higher at 26.7° C than at 93.4° C for any load condition. Higher efficiency means greater output for constant shaft torque input to the alternator.

Figure 9(a) displays the variation of armature temperature with inlet coolant temper-

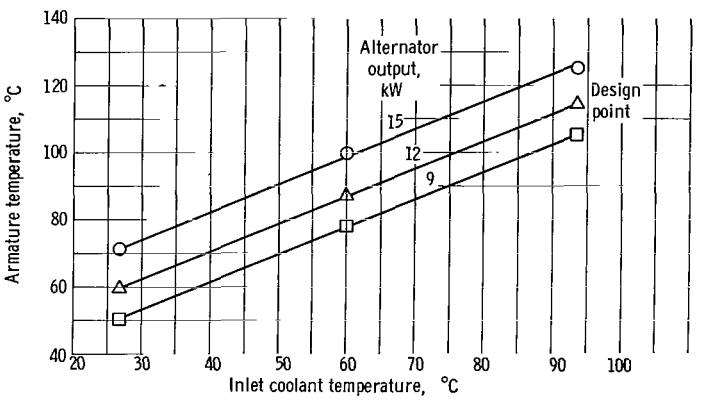

(a) Variation of armature temperature with inlet coolant temperature. Maximum design hot spot temperature, 180° C.

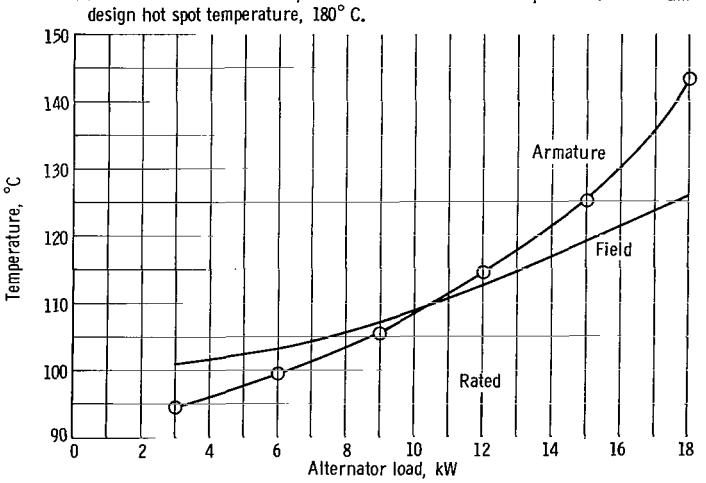

(b) Variation of armature and field temperature with alternator load. Inlet coolant temperature, 93.4° C.

Figure 9. - Temperature as function of coolant and load for 15-kilovolt-ampere Brayton-cycle alternator. Inlet coolant flow rate, 1.66 gallons per minute (6.3×10^{-3} m^3/min); 0.8 lagging power factor loads.

ature for a constant flow rate of 1.66 gallons per minute. Armature temperatures were measured within ±2.8° C of the test value using Chromel-Alumel thermocouples located on the armature winding end turns.

Inspection of figure 9(a) indicates that for design inlet coolant temperature (93.4° C) the alternator armature winding temperature is approximately 114.5° C. This temperature is lower than the maximum design hot-spot temperature of 180° C. At the off-design temperature of 26.7° C, an extrapolation of the data indicates that the alternator can continuously generate 2 per unit load. However, decreasing the system coolant temperature implies that the Brayton system radiator area and weight would have to be increased in order to dissipate the same amount of heat at lower temperature. Such an increase is generally undesirable. Therefore, it is important to maintain alternator losses as low as possible so that heat rejection requirements are minimized.

Figure 9(b) shows the variation of armature and field temperatures with alternator load at design inlet coolant temperature. These data demonstrate that the alternator has the thermal capacity to continuously generate 1.5-per-unit power output, therefore exceeding the overload requirements listed in table I.

Reactances and Time Constants

The reactances and time constants of the alternator were experimentally determined, so that the performance characteristics under transient or unbalanced load conditions could be predicted. They are listed in table III.

TABLE III. - REACTANCES AND TIME CONSTANTS

	Test	Calculated
Reactances, per unit:		
Direct-axis synchronous, X_d	1.16	1.259
Direct-axis transient, X'_d	.475	.381
Direct-axis subtransient, X''_d	.317	.361
Negative sequence, X_2	.308	.283
Zero sequence, X_0	.02	.015
Time constants, sec:		
Direct-axis transient, T'_d	.138	.1037
Direct-axis subtransient, T''_d	.003	.0050
Armature short circuit, T_a	.006	.0055
Direct-axis open circuit, T'_{do}	.48	.3890
Short-circuit ratio (SCR)	.89	.94

These constants are affected by magnetic saturation and, therefore, can have either a saturated or unsaturated value. Unless otherwise specified, the test values for the machine constants described in this paper are the saturated values. The alternator reactances and time constants were determined from short-circuit tests. In these tests the alternator was first operated open circuit with the field excitation required to produce rated terminal voltage provided by a dc power supply. Under these conditions, a balanced 3-phase short circuit was applied at the alternator terminals. The three armature phase currents and the field current were recorded oscillographically. An oscillogram of the short-circuit current is shown in figure 10. The short-circuit cur-

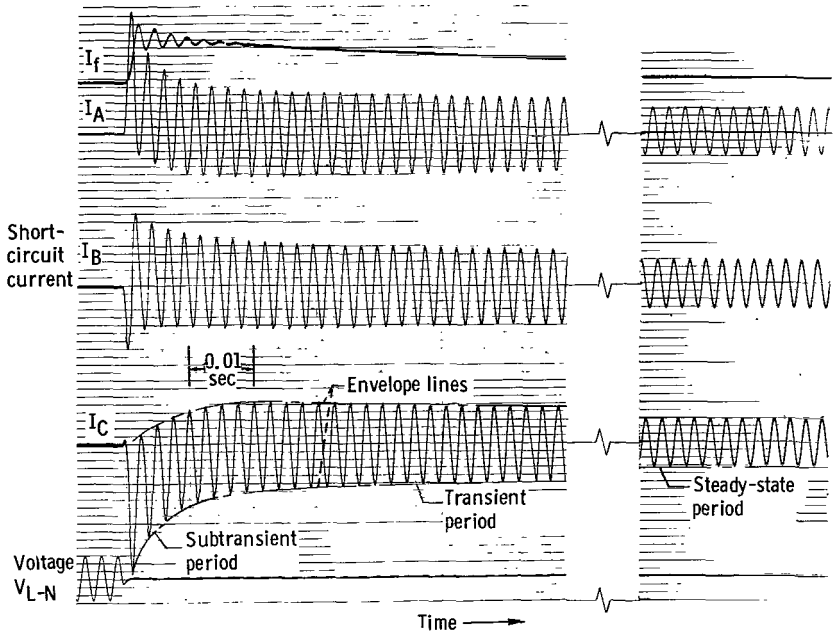

Figure 10. - Oscillogram of 3-phase sudden short circuit.

rent was analyzed for three time periods: (1) subtransient, (2) transient, and (3) steady-state.

According to Blondel's two-reaction theory (ref. 9) for conventional synchronous machines, there are two geometrical axes of symmetry - the direct and quadrature axes. From this theory, it is possible to represent this type of machine with a mathematical model and to analytically describe its behavior. Some of the quantities, such as direct- and quadrature-axis reactances which are used as mathematical tools to analyze a machine, do not physically exist within the machine.

One significant difference between a homopolar inductor machine and a conventional synchronous machine is their respective rotors. The inductor alternator homopolar rotor (fig. 2) does not have the symmetry that exists in the conventional machine. For the homopolar rotor, the polar and interpolar axes at one end are both direct axes. The bisector of the two direct axes is not an axis of symmetry and cannot be called a quadrature-axis as defined by classical terminology (ref. 10). However, since the inductor alternator has operating characteristics similar to that of a conventional synchronous machine, the quadrature-axis quantities are still used in technical literature for design and analysis. At present, not much work has been done in this area to change terminology and to develop methods of analysis which apply directly to inductor alternators. However, inductor alternators are being used in many aerospace applications.

In this report, only direct-axis quantities were measured. The quadrature-axis quantities were not measured, because they are neglected when analyzing the behavior of an alternator under short-circuit conditions. Under these conditions the power factor is theoretically zero, and the armature magnetomotive force is maximum along the direct-axis.

Direct-axis synchronous reactance. - Direct-axis synchronous reactance (X_d) can be defined as the ratio of the line-to-neutral rms voltage on the air-gap line (fig. 6(a)) to the armature current rms value on a sustained 3-phase short circuit for any given value of field current. The effect of armature resistance is neglected in the determination tion of X_d, because the resistance is small in comparison to the reactance. The per-unit unsaturated value for X_d was calculated by dividing this ratio by the system base ohms, where

$$\text{base ohms} = \frac{\text{rated line-to-neutral voltage}}{\text{rated line current}}$$

Direct-axis subtransient reactance. - The direct-axis subtransient reactance (X_d'') is the reactance which determines the initial rms value of the alternating current (ac) component of short-circuit current that flows in the armature winding upon the application of a sudden 3-phase short circuit at the alternator terminals. Figure 11(a) is a graphical analysis of the ac component of short-circuit armature current into the subtransient and transient currents. The method for obtaining the values for figure 11 is described in reference 8. The per-unit value of X_d'' was calculated from equation (1):

$$X_d'' = \frac{E}{I''} \tag{1}$$

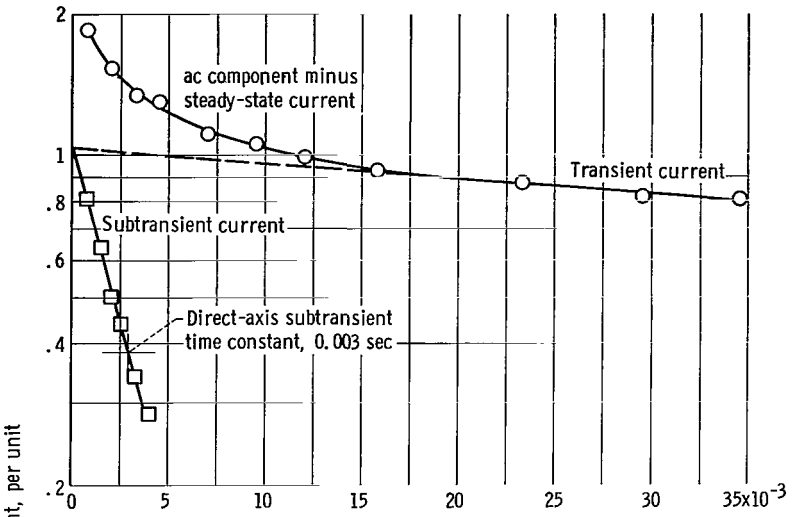

(a) Determination of direct-axis subtransient time constant.

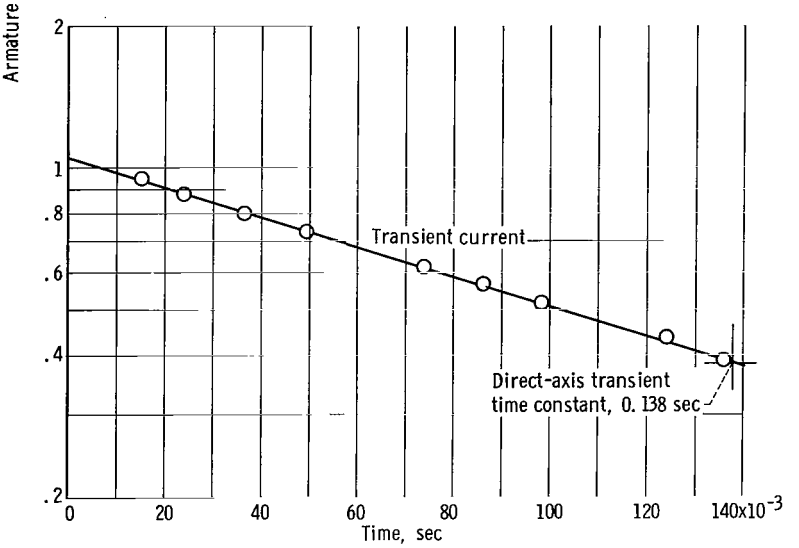

(b) Determination of direct-axis transient time constant.

Figure 11. - Analysis of alternating-current component of short-circuit armature current.

where

E per-unit open-circuit rms terminal voltage (L - N)

I'' per-unit initial ac short-circuit component (rms)

Direct-axis transient reactance. - The direct-axis transient reactance (X'_d) determines the maximum value of the rms short-circuit armature current that flows in the armature winding during the transient time period (as shown in fig. 10). Figure 11(b) shows the transient current of the ac component of short circuit. The per-unit value of X'_d was calculated from equation (2):

$$X'_d = \frac{E}{I'} \tag{2}$$

where

E per-unit rms open-circuit terminal voltage (L-N)

I' per-unit initial transient current plus steady-state current

Direct-axis subtransient time constant. - As illustrated in figure 11(a), the direct-axis subtransient time constant (T''_d) is the time required for the subtransient ac component of short-circuit current to decrease to 36.8 percent of its initial value. The subtransient period was graphically determined by subtracting the steady-state and transient currents from the total ac component. The resulting plot is approximately linear on the semilogarithmic paper. The experimental value for T''_d was 0.003 second. The subtransient portion of the ac waveform can be mathematically described as $I''_o e^{-t/T''_d}$, where I''_o is the initial value of the subtransient current after the application of the short circuit.

Direct-axis transient time constant. - The direct-axis transient time constant (T'_d) is the time required for the transient portion of short-circuit current to decrease to 36.8 percent of its initial value, as shown in figure 11(b). The transient period is indicated by the linear portion of the curve (fig. 11(a)) which represents the ac component minus the steady-state value. The straight line extension of the transient period to the vertical axis in figure 11(a) gives the initial value of the transient current on application of the short circuit. The direct-axis transient time constant T'_d equals 0.138 second and is long compared to T''_d (0.003 sec).

The transient portion of the ac waveform can be represented by $I'_o e^{-t/T'_d}$, where I'_o is the initial transient current on application of the short circuit. The resultant ac component (ref. 8) can be expressed as

$$I_{ac} = I_{ss} + I''_o e^{-t/T''_d} + I'_o e^{-t/T'_d}$$

$$= \frac{E}{X_d} + \left(\frac{E}{X''_d} - \frac{E}{X'_d}\right) e^{-t/T''_d} + \left(\frac{E}{X'_d} - \frac{E}{X_d}\right) e^{-t/T'_d}$$

Thus,

$$I_{ac} = 0.99 + 1.05\, e^{-333.3t} + 1.11\, e^{-7.25t}$$

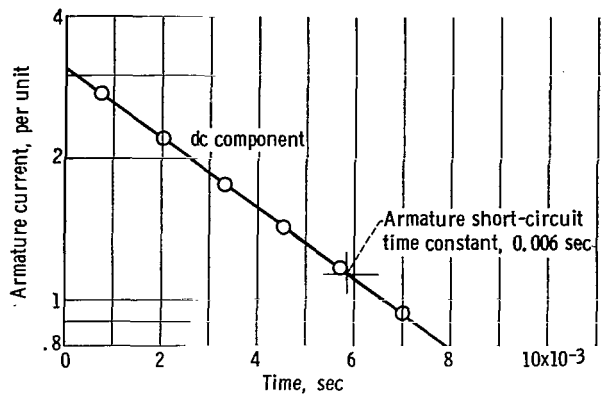

Figure 12. - Armature short-circuit time constant.

Neglecting the second term because of its relatively short duration,

$$I_{ac} \simeq 0.99 + 1.11\, e^{-7.25t}$$

In the foregoing calculations, the armature resistance and field resistance are neglected.

Armature short-circuit time constant and direct current component. - The armature short circuit time constant (T_a) shown in figure 12 is defined as the time required for the direct current component, of the short-circuit current waveform to decrease exponentially to 36.8 percent of its initial value. This dc component causes the current waveform to be asymmetrical as demonstrated in figure 10. In reference 11, an equation is given for the dc component of armature current

$$I_{dc} = \frac{\sqrt{2}\ E \cos \alpha}{X''_d}\ e^{-t/T_a}$$

where α is the switching angle and E is the open-circuit terminal voltage. Since the dc component is a function of the switching angle α, if $\alpha = 90^{\circ}$ at the instant the short circuit is applied, then no dc component is present, and the waveform is symmetrical. The oscillogram (fig. 10) shows that for the B-phase current trace, the waveform is almost symmetrical indicating that the switching angle approached 90° producing

a small dc component. The other two phases have relatively large dc components of approximately the same offset, but opposite in direction. This is expected because the other phases differ by 120° from B-phase and the algebraic sum of the dc components must be zero for balanced conditions.

Direct-axis open-circuit time constant. - The direct-axis open-circuit time constant (T'_{do}) is the time required for the transient component of the alternating voltage to decrease to 36.8 percent of its initial value as shown in figure 13. This time constant was

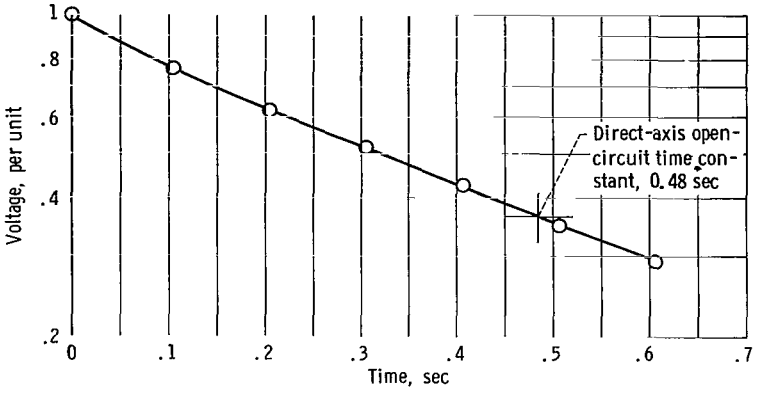

Figure 13. - Open-circuit transient time constant.

experimentally determined from test by suddenly shorting the field when the alternator was operating open circuit at rated terminal voltage. The decaying armature voltage was recorded oscillographically. The steady-state residual voltage was subtracted from the rms values of armature voltage on the oscillogram and the resulting points plotted against time in figure 13. In figure 13 one per-unit voltage is equal to 106 volts. The direct-axis open-circuit time constant, 0.48 second, is the largest time constant of the machine and is approximately four times greater than T'_d, the direct-axis time constant.

Zero sequence reactance. - The reactances discussed in this report were determined by applying a symmetrical 3-phase short circuit on the machine. Such a short circuit essentially represents a balanced load condition. For the case of an unbalanced load or short circuit on a machine, the method of symmetrical components (ref. 12) is usually applied to mathematically determine the resulting unbalanced currents and voltages. The components employed in this method are identified as positive, negative, and zero sequence. The following method of test was used to measure the zero sequence reactance

(X_0). The windings of the three armature phases were connected in series and a 400 hertz alternating voltage applied. The ratio of this applied voltage to three times the current gave the zero sequence impedance. The zero sequence resistance was determined from the measured power input (per phase) for this circuit. The per-unit zero sequence reactance (X_0) was then calculated by

$$X_0 = \sqrt{Z_0^2 - R_0^2}$$

where

Z_0 per-unit zero sequence impedance

R_0 per-unit zero sequence resistance

The zero sequence reactance for this machine is small (0.02 per unit). This is expected because this machine was designed with a 2/3 pitch of the armature coils (ref. 6). This design tends to reduce the zero sequence reactance.

Negative sequence reactance. - There are several methods of measuring negative sequence reactance (X_2). The method used for this machine is described in reference 8. This test is a line-to-line sustained short circuit at the alternator terminals at no-load and rated speed.

By test, X_2 was found to be 0.308 per unit. The calculated value is 0.283 per unit. The negative sequence reactance depends on the unbalanced load impedance applied to the alternator and as a result varies under different loading conditions (ref. 13). Since this test value of X_2 was determined by a short-circuit test, it is valid for the case of zero load resistance which occurs for most power system short circuits.

Short-Circuit Ratio

The short-circuit ratio is defined by the following ratio of two values of field current

$$\text{short-circuit ratio} = \frac{I_{FV}}{I_{FI}}$$

where

I_{FV} the field current required to produce rated open-circuit terminal voltage (L-N) at rated speed

I_{FI} the field current required for rated armature current on a sustained 3-phase short circuit

These values of field current were determined from the open circuit and 3-phase short-circuit saturation curves in figure 6(a). The short-circuit ratio thus obtained is 0.89 for this alternator.

The short-circuit ratio affects alternator performance. Typical values of short-circuit ratio range from 0.7 to 1.0. For a lower short-circuit ratio, a greater change in field current is required to maintain constant terminal voltage for a given change in load current (ref. 11).

Voltage Unbalance

A test was conducted to determine the effects of unbalanced loads on the balance of the 3-phase voltage of the alternator. The percent voltage unbalance is defined by

$$\text{percent unbalance} = \frac{\left|V_{avg} - V_{L-N}\right|_{max}}{V_{avg}} \times 100$$

where

V_{L-N} line-to-neutral voltage

V_{avg} the average of the three line-to-neutral voltages

Voltage unbalance results are summarized in table IV. The experimental data is compared with Brayton electrical system specifications listed in table I. It is evident from the test results that the alternator did not meet design goals for any unity power factor load. The reason for high values of voltage unbalance probably is the fact that the alternator was designed to maximize reliability and efficiency. Such design means a sacrifice in power quality requirements.

Voltage unbalance is affected by the negative sequence reactance (X_2). The design value for X_2 was 0.167 per unit, whereas the test value was 0.308 per unit. Since the experimental value of X_2 is significantly greater, the resulting voltage unbalance should be higher than expected. This condition is demonstrated by the data in table IV.

TABLE IV. - VOLTAGE UNBALANCE WITH UNBALANCED LOAD

Per-unit current[a]			Power factor, 1.0	Power factor, 0.8	Maximum voltage unbalance for 1.0 power factor (table I)
Aφ	Bφ	Cφ	Voltage unbalance, percent		
2/3	1	1	2.41	2.49	-
1/3	1	1	4.68	5.04	-
0	1	1	7.08	7.70	-
0	2/3	1	5.99	7.38	-
0	1/3	1	6.16	7.87	-
0	0	1	7.17	9.05	-
1/3	2/3	1	3.67	4.89	-
2/3	2/3	1	2.34	2.72	2
0	0	1/3	2.41	2.91	2
0	1/3	1/3	2.34	2.75	-
1/3	2/3	1/3	2.17	2.66	2
1/3	1	1/3	4.58	5.22	4
0	0	2/3	4.75	5.76	4
0	1/3	2/3	3.84	5.06	-
0	2/3	2/3	4.70	5.11	-
1/3	2/3	2/3	2.25	2.49	-

[a]1 Per-unit current, 41.7 A.

The maximum voltage unbalance is 9.05 percent with a single-phase load at 0.8 lagging power factor and rated armature current.

Short-Circuit Tests

The objective of these tests was to verify alternator short-circuit capacity specifications. For this testing, the Brayton voltage regulator-exciter (ref. 6) supplied the required field excitation. Table V summarizes the various faults applied at the terminals of the alternator-voltage regulator combination. NASA and manufacturer test data are compared, and the results indicate good correlation. These data show that the alternator exceeds short-circuit current specifications listed in table I.

The alternator input shaft torque was also measured for each fault. The torque for any fault applied exceeded 0.5 per-unit full-load torque. This information is important in the design of protection against turbine overspeed, because a fault at the alternator terminals could remove the effect of the parasitic speed control in the Brayton cycle system.

TABLE V. - SHORT-CIRCUIT TESTS

Type of fault[a]	NASA test[b]		Manufacturer's test
	Fault current,[c] per unit	Torque,[d] per unit	Fault current, per unit
L-N	5.67	0.84	6.13
L-L	3.09	.59	3.13
L-L-N	6.20	.96	----
L-L-L	4.42	.72	4.11
L-L-L-N	4.43	.74	----

[a]Each fault was applied for 5 sec.

[b]Lead resistance per phase to fault, 0.005 ohm.

[c]1 Per-unit fault current, 41.7 A.

[d]1 Per-unit full load torque, 7.64 lb-ft (10.35 N-m).

Harmonic Analysis

Flight system vehicle loads, such as sensitive electronic equipment, will require an input signal having low harmonic distortion. In order to predict the distortion of the alternator waveforms, a harmonic analysis was performed on the line-to-neutral voltage and the line current for various linear loads. (A linear load is defined as an impedance that does not change with a variation in applied voltage.)

The individual harmonics at each load condition were measured with a wave analyzer and a X-Y recorder. The input signal to the wave analyzer was either the line-to-neutral voltage or the output signal from a special current transformer, suitable for high frequencies, which provided a signal directly proportional to the line current. Individual harmonics presented in tables VI and VII were measured with the wave analyzer in percent relative to the fundamental (100 percent). Frequencies as high as 16.4 kilohertz were measured, so that the slot harmonic (twenty-fifth) which occurs at 10 kilohertz was included.

The data in table VI indicates that the strongest individual harmonic is the fifth harmonic at rated load. For loads less than 9 kilowatts, the twenty-fifth is strongest. This

TABLE VI. - VOLTAGE HARMONICS

FOR LINEAR LOADS

[All voltage harmonics are for line-to-neutral voltages.]

(a) Alternator load, open circuit

Harmonic order, i	Amplitude, percent
3	0
5	2.541
7	2.148
9	0
11	.246
13	.708
15	0
17	0
19	.532
21	0
23	.791
25	5.552
27	0
29	.348
31	0
33	0
35	.120
37	0
39	0
41	.150
Total harmonic content, percent	6.597

twenty-fifth harmonic exceeds 3 percent for an output less than 6 kilowatts. This condition does not meet the design goal (table I) of 3 percent maximum - no load to full load. However, for the normal operating range of the alternator (9 to 12 kW) this harmonic is less than 3 percent. Only odd harmonics are given in tables VI and VII; no even harmonics exist because of the symmetry of alternator construction.

The total harmonic content was calculated by

TABLE VI. - Concluded. VOLTAGE HARMONICS FOR LINEAR LOADS

(b) Power factor, 1.0

Harmonic order, i	Alternator load, kW						
	1.5	3.0	6.0	9.0	12.0	15.0	18.0
	Amplitude, percent						
3	0	0	0.054	0.071	0.093	0.088	0.110
5	2.515	2.396	2.101	2.044	1.916	1.794	1.620
7	1.807	1.419	.852	.667	.692	.686	.711
9	0	0	.018	.036	.036	.082	.149
11	.274	.100	.309	.484	.492	.462	.409
13	.551	.412	.157	.307	.367	.351	.345
15	0	0	0	.042	.060	.074	.096
17	0	.100	.060	.259	.262	.193	.115
19	.403	.394	.143	.215	.257	.204	.124
21	0	0	0	.054	.063	.030	0
23	.403	.170	.282	.235	.387	.356	.118
25	4.716	3.667	2.413	1.881	1.589	1.272	1.044
27	.026	.038	.040	.068	.082	.068	.080
29	.280	.238	.092	.066	.162	.182	.120
31	.039	.104	.040	.060	.110	.097	.062
33	.002	.015	.017	.024	.015	.014	.017
35	.141	.135	.098	.039	.063	.044	.039
37	.036	.045	.052	.039	.066	.055	.035
39	0	.007	.016	0	.006	.018	.012
41	.176	.113	.106	.063	.030	.045	.034
Total harmonic content, percent	5.716	4.655	3.350	2.948	2.722	2.434	2.149

(c) Power factor, 0.8

Harmonic order, i	Alternator load, kW						
	1.5	3.0	6.0	9.0	12.0	15.0	18.0
	Amplitude, percent						
3	0	0	0.054	0.132	0.157	0.223	0.210
5	2.506	2.321	2.056	1.973	1.852	1.760	1.594
7	1.788	1.413	.863	.724	.636	.639	.614
9	0	.090	.057	.048	.030	.021	.027
11	.246	.150	.260	.329	.370	.392	.387
13	.542	.423	.187	.090	.176	.257	.282
15	0	0	.024	.012	.006	.021	.030
17	0	.060	.036	.068	.151	.201	.212
19	.403	.377	.187	.113	.124	.176	.199
21	0	0	0	0	.009	.036	.039
23	.440	.259	.337	.345	.204	.093	.036
25	4.836	3.674	2.468	2.131	1.742	1.504	1.320
27	.031	.030	.054	.036	.045	.066	.096
29	.295	.259	.113	.030	.021	0	.064
31	.038	.060	.030	0	0	.012	.053
33	.005	0	.024	.015	.006	.012	.033
35	.135	.120	.110	.063	.042	.054	.067
37	.038		.060		0	.015	.041
39	.003		.024		0	0	.018
41	.167		.102		.030	.036	.041
Total harmonic content, percent	5.806	4.625	3.371	3.039	2.674	2.476	2.247

TABLE VII. - CURRENT HARMONICS FOR LINEAR LOADS

(a) Power factor, 1.0

Harmonic order, i	Alternator load, kW						
	1.5	3.0	6.0	9.0	12.0	15.0	18.0
	Amplitude, percent						
3	1.567	1.234	1.061	1.100	1.219	1.107	1.143
5	2.203	1.567	1.356	1.326	1.406	1.325	1.264
7	1.449	2.042	.966	.473	.192	.017	.067
9	.632	.589	.525	.506	.456	.338	.310
11	.395	.298	.100	.143	.217	.238	.238
13	.350	.749	.279	.075	.070	.138	.162
15	.286	.220	.252	.247	.159	.150	.195
17	.160	.186	.057	.042	.086	.105	.083
19	.210	.347	.143	.042	.073	.132	.138
21	.259	.120	.143	.154	.067	.067	.098
23	.686	.298	.372	.301	.283	.274	.226
25	3.783	3.048	1.963	1.465	1.313	1.113	.864
27	.468	.238	.135	.102	.057	0	.030
29	.335	.210	.078	.033	.040	.077	.092
31	.177	.129	.048	.015	0	.007	0
33	.108	.129	.042	.045	.043		.017
35	.083	.063	.015	.015	0		
37	.060	.060	0	0	0		
39	.067	.092	.021	.006	.020		
Total harmonic content, percent	5.048	4.346	2.897	2.411	2.369	2.132	1.992

(b) Power factor, 0.8

Harmonic order, i	Alternator load, kW						
	1.5	3.0	6.0	9.0	12.0	15.0	18.0
	Amplitude, percent						
3	1.222	0.835	0.854	0.925	0.898	0.813	0.825
5	1.676	1.119	1.037	1.034	.995	.946	.898
7	1.249	1.481	1.010	.758	.531	.438	.404
9	.486	.385	.399	.441	.428	.371	.338
11	.305	.198	.097	.092	.105	.098	.089
13	.314	.546	.339	.244	.138	.098	.067
15	.220	.143	.151	.195	.195	.168	.135
17	.130	.110	.048	.050	.037	.030	.013
19	.180	.244	.149	.123	.086	.073	.060
21	.200	.097	0	.073	.092	.073	.053
23	.595	.315	.350	.353	.280	.204	.123
25	3.120	2.247	1.789	1.403	1.128	.949	.810
27	.365	.162	.083	.067	.063	.040	.020
29	.283	.143	.066	.047	.057	.060	.037
31	.141	.083	.054	.033	.040	.027	.010
33	.089	.069	0	.017	.007	.007	.007
35	.067	.012	.066	.020	.020	.023	
37		.027					
39		.036					
Total harmonic content, percent	4.094	3.153	2.549	2.219	1.925	1.701	1.573

$$\text{Percent total harmonic content} = \sqrt{\sum_{i=3}^{41} A_i^2}$$

where A_i is percent of the i^{th} odd harmonic relative to the fundamental. The slot harmonic represents 84 percent of the total harmonic content at no load and decreases with increasing load to 65 percent of the harmonic content at rated load. This harmonic could have been eliminated by skewing the stator. But since this method of design would have resulted in reduced alternator reliability, this technique was not used (ref. 6).

Figure 14(a) is a graphical representation of total harmonic content for unity power factor loads. Total current harmonic content is slightly less than the voltage harmonic content for any alternator load. Theoretically, the current and voltage waveforms should have identical shapes, and hence the same total harmonic content at any unity power factor load. However, the experimental system feeder lines and current transformers have inductance which tends to reduce high-frequency current harmonics. The

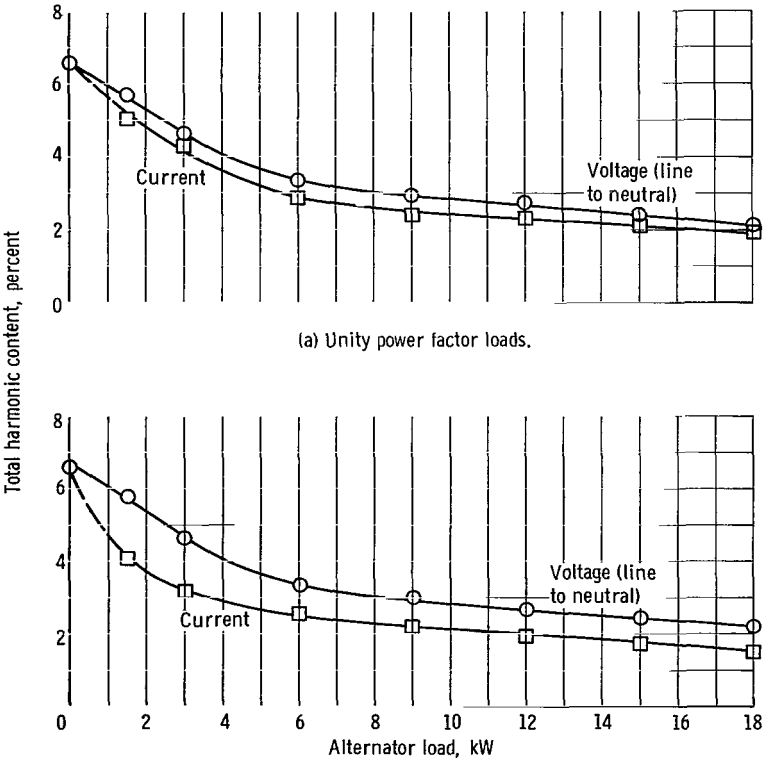

Figure 14. Waveform total harmonic content for linear loads for 15-kilovolt-ampere Brayton-cycle alternator.

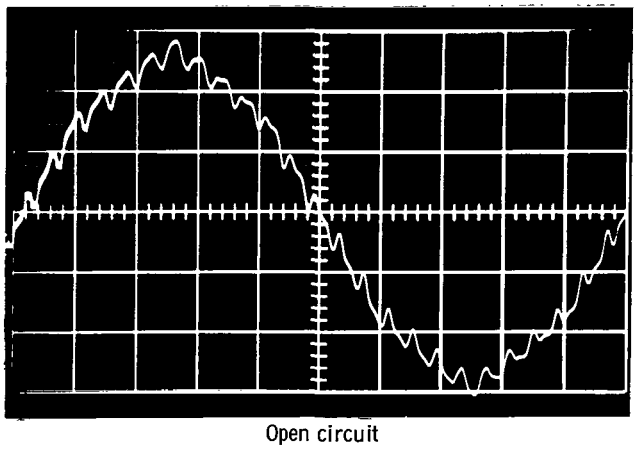

Open circuit

Line-to-neutral voltage

Line current

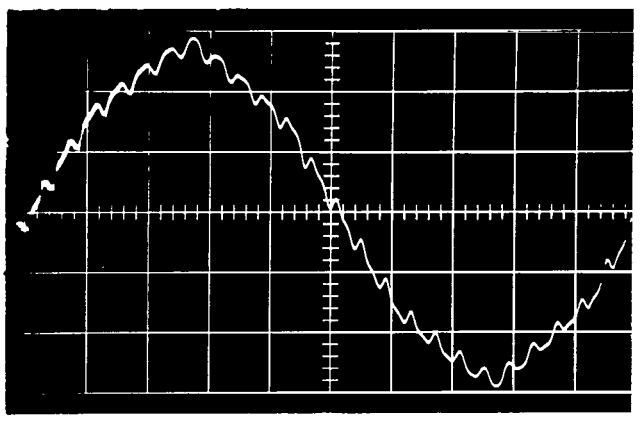

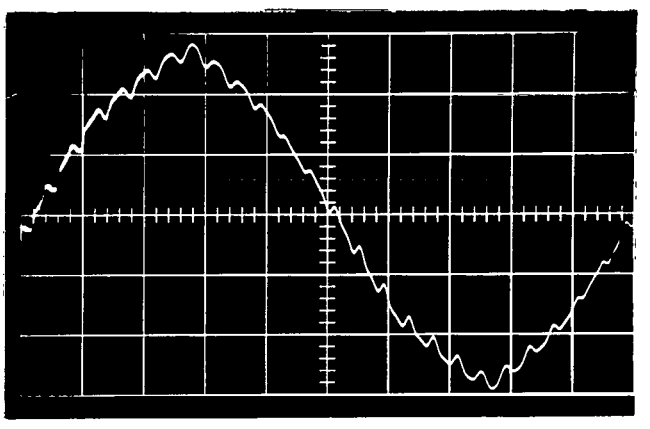

1.5 kw

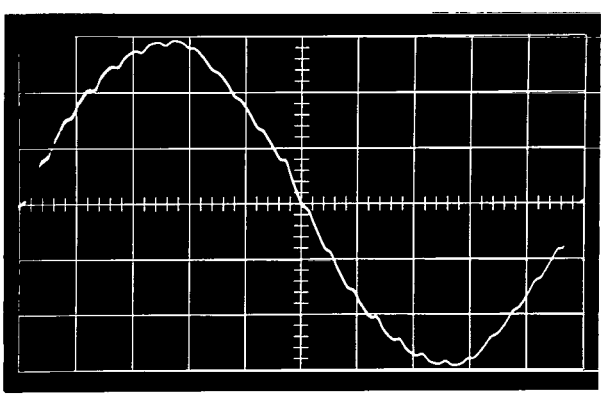

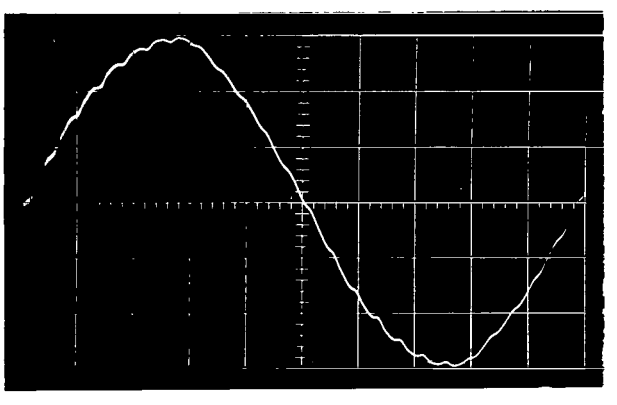

12 kw

(a) At unity power factor.

Figure 15. - Alternator waveforms for linear loads. Uncalibrated photographs.

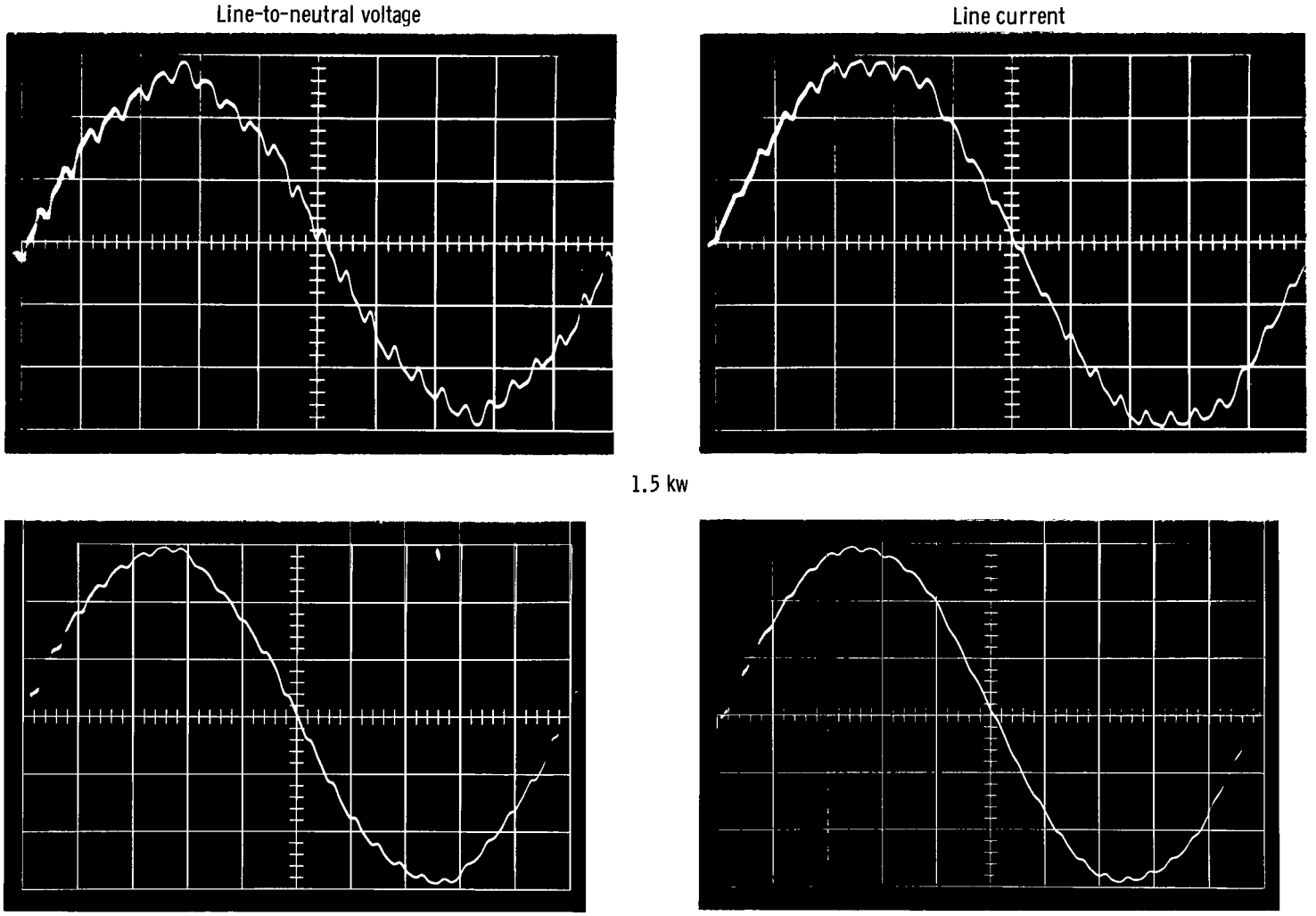

(b) At 0.8 lagging power factor.

Figure 15. - Concluded.

total harmonic content is less than 3 percent in the range from 9 to 18 kilowatts. Results at any unity power factor load are lower than the system design goal (table I) of 7 percent maximum harmonic content.

Figure 14(b) shows the variation in total harmonic content at 0.8 lagging power factor loads. For a given power load, current harmonic content is less for an 0.8 lagging power factor load than for a unity power factor load. This effect is due to the inductive load reactance which increased suppression of high-frequency current harmonics. At rated load, the voltage harmonic content is 2.67 percent and the waveform approaches a sinusoid.

Uncalibrated photographs of the voltage and current waveforms are shown in figures 15(a) and (b) to illustrate their characteristic shapes.

SUMMARY OF RESULTS

Test of the 15 kilovolt ampere homopolar inductor alternator produced the following results:

1. The alternator tested has the electromagnetic capacity to generate 2 per-unit rated output without significant saturation.

2. At design inlet coolant temperature, the alternator has the thermal capacity to continuously generate 1.5 per-unit rated output thus exceeding overload requirements.

3. Alternator efficiency has a peak value of 91.8 percent for an output of 11.25 kilovolt amperes. This agrees with design goals. At the rated output of 15 kilovolt amperes, efficiency is 91.5 percent. Efficiency exceeds 90 percent for outputs from 4 to 15 kilovolt amperes at unity power factor.

4. For an off-design inlet coolant temperature of 26.7° C, alternator efficiency is 92 percent at rated output. At this temperature, the alternator could continuously deliver 2 per-unit rated output.

5. The alternator did not meet voltage unbalance specifications for any unity-power-factor load.

6. The alternator exceeds short-circuit capacity specifications.

7. For any combination of short-circuit faults applied at the alternator terminals, the alternator input shaft torque exceeded 0.5 per-unit full-load torque. This performance is important in the design of protection against turbine overspeed, because a fault at the alternator terminals could otherwise remove the effect of the parasitic speed control in the Brayton cycle system.

8. Line-to-neutral voltage total harmonic content is 2.67 percent for rated output. For any unity-power-factor linear load, the total harmonic content is less than 7 percent and satisfies design goals.

9. The highest individual harmonics are the fifth and twenty-fifth. For alternator output less than 0.5 per unit, the twenty-fifth harmonic exceeds the design goal of 3 percent maximum. However, for rated output of 15 kilovolt amperes, the maximum harmonic (fifth) is 1.85 percent and meets design goals.

10. Windage losses were about 50 percent lower than design predicted, probably as a result of the windage baffles.

Lewis Research Center,
National Aeronautics and Space Administration,
Cleveland, Ohio, April 12, 1968,
120-27-03-42-22.

APPENDIX - INSTRUMENT SPECIFICATIONS

True RMS Voltmeter (6)

Voltage range:	100 μV to 320 V rms
Accuracy:	±3 percent from 15 to 150 kHz calibrated to within ±1 percent at 400 Hz
Input impedance:	10 megohms shunted by 18 pf

Digital Voltmeter (3)

DC voltage range:	±0 to 999.99 V
Accuracy:	±0.01 percent of reading or 1 digit, whichever is greater (10^{o} to 40^{o} C)
Input impedance:	Greater than 10 megohms

AC-DC Converter (3)

Input voltage range:	0 to 1099.9 V
Accuracy:	±0.25 percent of full scale
Frequency response:	60 Hz to 5 kHz
Input impedance:	Greater than 1 megohm
Output voltage range:	±0 to 10.999 V

Wave Analyzer (1)

Voltage range:	30 μV to 300 V
Frequency range:	20 Hz to 50 kHz
Accuracy:	±(1 percent + 5 Hz) ±5 percent of full-scale voltage
Input Impedance:	100 000 ohms or greater

True RMS Wattmeter (3)

Input voltage:	50 V, 100 V, 200 V (nominal)
Input current:	5 A (nominal)
Accuracy:	±1 percent of full scale
Frequency response:	dc to 2500 Hz

X-Y Recorder (1)

Accuracy:	±0.15 percent of full scale (static) ±0.2 percent at 10 in./sec (dynamic)

Oscillograph (1)

Recording channels:	24
Frequency range:	0 to 5000 Hz/sec (depends on type of galvanometer used)
Linearity:	±2 percent of reading with deflection of 4 in. or less

Oscilloscope (1)

Input impedance:	1 megohm paralled by 47 $\mu\mu$f
Bandpass:	dc - 450 kHz
Sweep rate:	1 microsecond to 5 seconds per centimeter, accuracy within 1 percent of the indicated sweep rate
Sensitivity:	1 millivolt to 20 volts per centimeter, accurate within 3 percent

Electronic Counter (1)

Frequency range:	10 Hz to 1.2 MHz
Accuracy:	±1 count ± time base accuracy
Input sensitivity:	0.1 to 150 V rms
Input impedance:	approximately 1 megohm, 50 pf shunt

Transducer Amplifier and Differential Transformer Unit (1)

Indicator accuracy:	1 percent of scale
Sensitivity:	±0. 100 inch to ±0. 0001 inch, full scale

Force Transducer (1)

Load cell range:	±100 pounds
Linearity:	0. 2 percent of range

Strip-Chart Recorder (1)

Accuracy:	±0. 25 percent of full-scale span or 20 microvolts, whichever is greater
Dead-band:	0. 1 percent of full-scale span

Precision True RMS Voltmeter (1)

Voltage range:	0. 1 to 1199. 9 V
Frequency range:	50 Hz to 20 kHz
Accuracy:	1/4 percent (100 Hz to 10 kHz; 0. 1 to 300 V)
Input impedance:	2 megohms

REFERENCES

1. Hurrell, Herbert G.; and Thomas, Ronald L.: Control and Startup Considerations for Two-Spool Solar-Brayton Power System. NASA TM X-1270, 1966.
2. Tew, Roger C.; Gerchman, Robert D.; and Hurrell, Herbert G.: Analog-Computer Study of Parasitic-Load Speed Control for Solar-Brayton System Turboalternator. NASA TN D-3784, 1967.
3. Thomas, Ronald L.: Turboalternator Speed Control with Valves in Two-Spool Solar-Brayton System. NASA TN D-3783, 1967.
4. Stewart, Warner L.; Glassman, Arthur J.; and Krebs, Richard P.: The Brayton Cycle for Space Power. Paper No. 741 A, SAE, Sept. 1963.
5. Glassman, Arthur J.; and Stewart, Warner L.: A Look at the Thermodynamic Characteristics of Brayton Cycles for Space Power. Paper No. 63-218, AIAA, June 1963.
6. Dryer, A. M.; Kirkpatrick, F. M.; Russell, E. F.; Wimsatt, J. M.; and Yeager, L. J.: Alternator and Voltage Regulator-Exciter Design and Development. Vol. I. General Electric Co., June 9, 1967.
7. Ellis, J. N.; and Collins, F. A.: Brushless Rotating Electrical Generators for Space Auxiliary Power Systems. Vol. I. Lear Siegler, Inc. (NASA CR-54320), Apr. 26, 1965.
8. Anon.: Test Procedures for Synchronous Machines. No. 115, IEEE, Mar. 1965.
9. Doherty, R. E. and Nickle, C. A.: Synchronous Machines. I. An Extension of Blondel's Two-Reaction Theory. AIEE Trans., vol. 45, June 1926, pp. 912-947.
10. Erdélyl, E. A.; Trutt, F. C.; and Hopkins, R. E.: Saturated High-Speed Homopolar Alternators at Balanced Loads. IEEE Trans. on Aerospace, vol. AS-2, no. 2, Apr. 1964, pp. 929-936.
11. Kimbark, Edward W.: Power System Stability. Vol. III. John Wiley & Sons, Inc., 1956.
12. Clarke, Edith: Circuit Analysis of A-C Power Systems. Vol. I. John Wiley & Sons, Inc., 1943.
13. Thomas, W. A.: Negative-Sequence Reactance of Synchronous Machines. AIEE Trans., vol. 55, Dec. 1936, pp. 1378-1385.

NASA-Langley, 1968 —— 3 E-4377

NATIONAL AERONAUTICS AND SPACE ADMINISTRATION
WASHINGTON, D. C. 20546

OFFICIAL BUSINESS

FIRST CLASS MAIL

POSTAGE AND FEES PAID
NATIONAL AERONAUTICS AND
SPACE ADMINISTRATION

POSTMASTER: If Undeliverable (Section 158 Postal Manual) Do Not Return

"The aeronautical and space activities of the United States shall be conducted so as to contribute . . . to the expansion of human knowledge of phenomena in the atmosphere and space. The Administration shall provide for the widest practicable and appropriate dissemination of information concerning its activities and the results thereof."

—NATIONAL AERONAUTICS AND SPACE ACT OF 1958

NASA SCIENTIFIC AND TECHNICAL PUBLICATIONS

TECHNICAL REPORTS: Scientific and technical information considered important, complete, and a lasting contribution to existing knowledge.

TECHNICAL NOTES: Information less broad in scope but nevertheless of importance as a contribution to existing knowledge.

TECHNICAL MEMORANDUMS: Information receiving limited distribution because of preliminary data, security classification, or other reasons.

CONTRACTOR REPORTS: Scientific and technical information generated under a NASA contract or grant and considered an important contribution to existing knowledge.

TECHNICAL TRANSLATIONS: Information published in a foreign language considered to merit NASA distribution in English.

SPECIAL PUBLICATIONS: Information derived from or of value to NASA activities. Publications include conference proceedings, monographs, data compilations, handbooks, sourcebooks, and special bibliographies.

TECHNOLOGY UTILIZATION PUBLICATIONS: Information on technology used by NASA that may be of particular interest in commercial and other non-aerospace applications. Publications include Tech Briefs, Technology Utilization Reports and Notes, and Technology Surveys.

Details on the availability of these publications may be obtained from:

SCIENTIFIC AND TECHNICAL INFORMATION DIVISION

NATIONAL AERONAUTICS AND SPACE ADMINISTRATION

Washington, D.C. 20546